

In the field of modern scientific-grade Charge Coupled Devices (CCDs) detectors the arrival of back-illuminated CCDs and Electron-Multiplying Charge Coupled Devices (EMCCDs) has offered key enabling technology for the growing range of applications where the photon signal available is extremely low. Such applications include low-light cell microscopy and fast chemical mapping. This document presents one of the key challenges associated with the use of back-illuminated, CCDs for Near-Infrared (NIR) detection, namely optical etaloning, and outlines with particular reference to a manufacturing process called ‘fringe suppression’.

Introduction

The ability of a CCD camera to capture photons and ‘detect’ the associated ‘photoelectrons’ that are generated is typically measured in terms of signal-to-noise ratio (SNR). The SNR can be expressed as follows:

$$SNR = \frac{QE \cdot P}{\sqrt{\left(\frac{N_{RN}}{G}\right)^2 + F^2 \cdot (N_{DN}^2 + N_{CIC}^2 + N_{SN}^2)}} \quad [i]$$

Where **QE** (Quantum Efficiency) is the probability of an incoming photon being absorbed in the photosensitive region of the sensor, **N_{RN}** the readout noise of the sensor, **N_{DN}** its dark noise, **N_{CIC}** the noise associated with clocking induced charge (CIC) and **N_{SN}** the shot noise associated with the incoming photon signal [1]. **P** denotes the photon flux of the signal incident on the pixel, **G** is the gain or multiplication factor should an EMCCD be used, and **F** denotes the Noise Factor. The noise factor takes into account the fact that in the case where Gain is applied to a raw signal to amplify it, the input noise to the amplification stage is also amplified.

It is clear that achieving high **SNR** depends not only on careful minimization of the different sensor noise sources (cooling for the dark noise, slower readout speed and/or use of electron multiplying gain for the readout noise, fast vertical clocking for CIC), but also on high sensor QE.

Back-illumination of CCDs – the attraction of high Quantum Efficiency in the Visible and NIR Regions

The QE of a CCD is governed by its ability to absorb incoming photons in the photosensitive silicon also known as the depletion region. It is only in this region that photons are converted into electron-hole pairs,

which are then confined by means of electric fields into a ‘pixel’. The charges held in these pixels can then be read out.

Shorter wavelength photons (blue light) are absorbed closer to the silicon surface, while longer wavelength photons can travel deeper into the silicon matrix before being absorbed. Photons with wavelength above 1.1 μm do not have enough energy to create an electron-hole pair and so cannot be detected: a silicon CCD is effectively transparent at these longer wavelengths.

Figure 1 shows the absorption depth of photons as a function of wavelength in crystalline silicon.

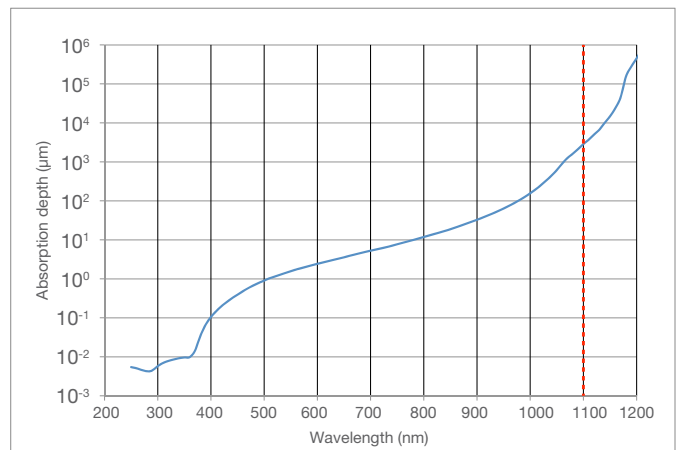


Figure 1: Absorption depth in Silicon at 300K as a function of incident photon wavelength^[1]

In front-illuminated CCDs, incoming photons must first transverse a polysilicon electrode structure and a silicon oxide (SiO) insulating layer (see Figure 2). The electrode structure can absorb and reflect part of the incoming photon flux before it reaches the photosensitive region. This region is also referred to as the depletion region (it is depleted in mobile charge carriers) and has the ability to capture and store the electrons generated from the photon signal.

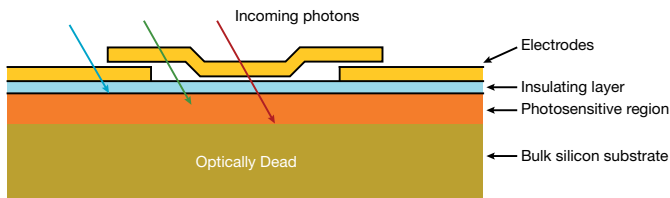


Figure 2: Typical front-illuminated CCD (cross section)

This absorption in the surface layers is extremely pronounced in the ultraviolet (<350 nm), resulting in near zero detection for UV photons. This design structure also limits the QE of front illuminated devices to ~50% in the visible.

In order to eliminate the losses incurred at the front surface, a back-illuminated (BI) configuration can be adopted. The back-illumination process involves the removal of the bulk silicon substrate by mechanical grinding and chemical etching, allowing direct exposure of the active photosensitive region to the incoming photons as shown on Figure 3. These devices can exhibit peak QE's of up to 95% with appropriate anti-reflection (AR) coatings. NIR QE of standard back-illuminated CCDs can be further enhanced by the use of a thicker photosensitive region, also referred to as the **deep depletion** region. Material with higher resistivity is used in these devices.

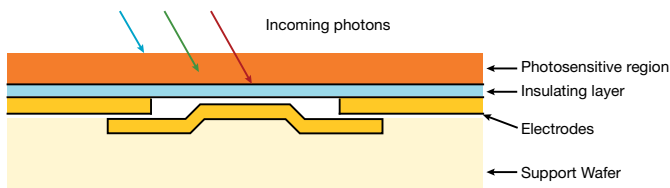


Figure 3: Typical back-illuminated CCD (cross section)

- The thicker photosensitive region offers a greater absorption path to longer wavelength photons, and subsequently lowers the probability for these photons

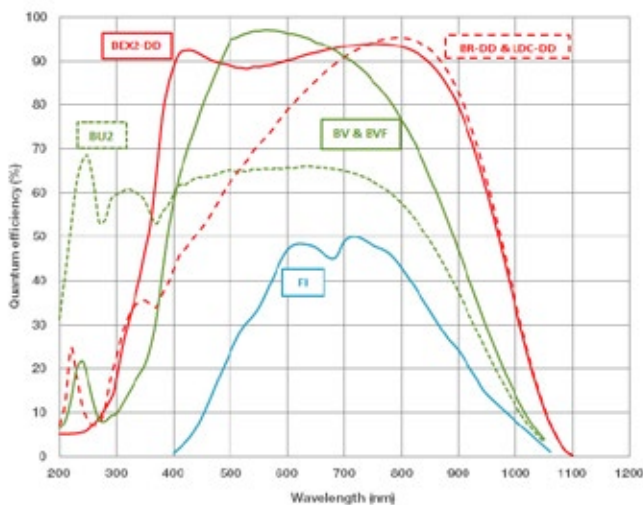


Figure 4: Typical QE performance at +25°C of front-illuminated ('FI'), back-illuminated visible-optimized ('BV'), UV-enhanced back-illuminated ('BU2'), back-illuminated deep-depletion CCDs with NIR AR-coating ('BR-DD') and broadband dual AR-coating ('BEX2-DD'). The new BI Low Dark Current Deep-Depletion ('LDC-DD')¹⁴ and 'BR-DD' have identical QE characteristics.

transversing the whole way across the active region (refer to Figure 1).

- The higher resistivity material allows the electric fields, created by applying voltages to the electrodes, to penetrate the entire depth of the now thicker photosensitive region and hence better collect and confine photoelectrons within the pixels.

These devices are known as back-illuminated, deep-depletion (BI-DD) CCDs.

A property of back-illuminated CCDs that is often overlooked is their propensity to generate constructive and destructive optical interference when illuminated with coherent photons. This behavior is especially pronounced in the NIR and can lead to signal modulation as high as 40%. This highly undesirable effect can be extremely disruptive for applications based on NIR Raman, NIR photoluminescence or Bose Einstein Condensate (BEC) studies.

Front-illuminated CCDs however, do not suffer from optical etaloning. In these devices, incoming photons with longer absorption lengths (longer wavelengths) do not encounter any interface with highly mismatch refractive indexes after reaching the photosensitive region. These photons have therefore a very low chance of being reflected back-and-forth in the depletion region and create interferences. Photons that are not absorbed in this region are lost in the optically dead bulk silicon substrate.

The following section describes the origin of the interferometer behavior of back-illuminated CCDs, by comparing their structure with a particular type of interferometer called a Fabry-Pérot étalon.

The ultra-thin cavity formed by the depletion region, with parallel and highly reflective surfaces is akin to a Fabry-Pérot étalon configuration.

Back-illuminated CCDs and analogy to the Fabry-Pérot étalon

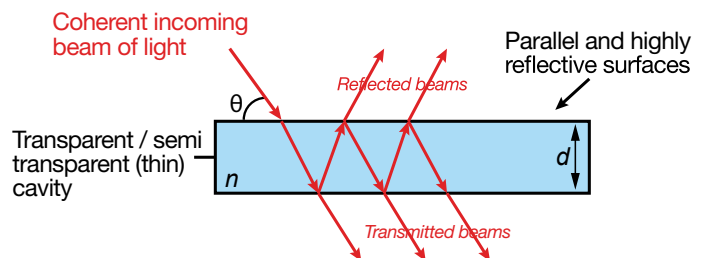


Figure 5: Typical Fabry-Pérot étalon configuration

A typical Fabry-Pérot étalon consists of a thin, transparent optical medium with two flat, parallel and highly reflective surfaces. A back-illuminated CCD is akin to this configuration, with the depletion region sandwiched between a silicon oxide insulating layer and air / vacuum with highly mismatched refractive indexes

which create highly reflective interfaces. Coherent light entering the cavity can undergo multiple reflections, which can lead to the generation of destructive and constructive interference, largely determined by the Etalon configuration in terms of its thickness or ‘optical length’, and the dielectric properties of the material within it. This is illustrated in Figure 7.

The modulation characteristics of the signal are governed by the following equation (adapted from [3]):

$$T = \left[\frac{1}{1 + \left(\frac{2F}{\pi}\right)^2 \sin^2\left(\frac{\varphi}{2}\right)} \right] \quad \text{[ii]}$$

$$\text{with } F \approx \frac{n\sqrt{R}}{(1-R)} \text{ and } \varphi = \frac{2\pi}{\lambda} 2nd \cos\theta \quad \text{[iii]}$$

where **T** is the transmittivity function of the étalon, **F** is a measure of the quality of the étalon known as Finesse, **R** is the reflectivity of the étalon surfaces (assumed to be identical for simplification), **φ** the roundtrip phase change of the photon signal, **n** the refractive index of the cavity medium, **d** the distance between the étalon surfaces and **θ** the angle of the incoming light relative to the étalon surface. Figure 6 shows the influence of the cavity Finesse on the quality of the étalon.

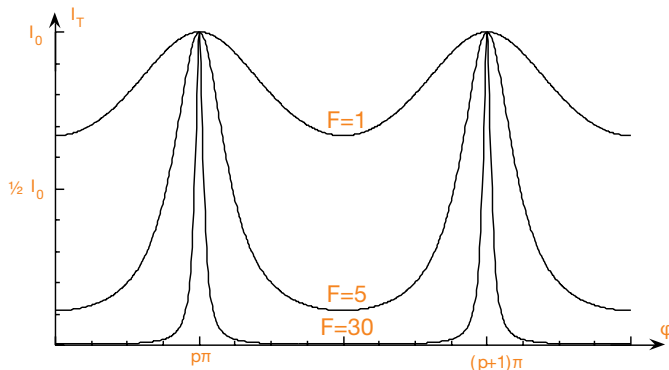


Figure 6: Influence of cavity Finesse on fringing sharpness and amplitude (integers p and p+1 refer to consecutive fringes separated by one roundtrip through the cavity)

Etalons with highly reflective surfaces (high R, hence high Finesse) show sharper transmission peaks, while etalons with less reflective surfaces (low R, hence low Finesse) lead to increasingly smeared fringes.

The spacing in wavelength between two successive transmitted optical intensity maxima of a Fabry-Pérot étalon is given by the **free spectral range (FSR)**. Typical FSR values for back-illuminated CCDs are shown below:

- Back-illuminated visible-optimized CCDs: FSR ~5 - 10 nm for photons in the 700 - 1100 nm region,
- Back-illuminated deep-depletion CCDs: FSR ~2 - 4 nm for photons in the 700 - 1100 nm region

Spectral and spatial etaloning in back illuminated CCDs

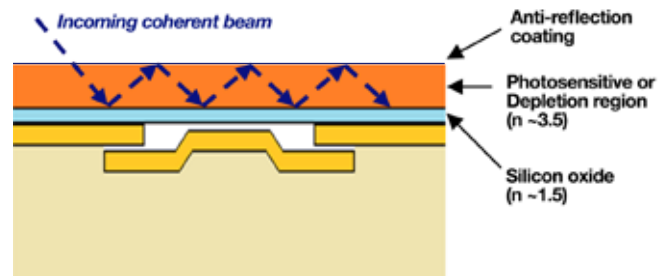


Figure 7: Back-illuminated, sensor and étalon cavity structure analogy (n refers to the refractive index)

The thickness of the depletion region in back-illuminated CCDs can typically vary between 10-50 μm (type-dependent). The absorption length of NIR photons in silicon can be several times this thickness (see Figure 1), which effectively means that the CCD is semi-transparent at these wavelengths. The CCD depletion region has a refractive index of ~3.5, while the silicon oxide (insulating) layer has a refractive index of ~1.5. This significant mismatch means that this interface is extremely reflective, so that NIR photons entering the depletion region and reaching the insulating layer without being absorbed will be reflected back towards the front surface of the depletion region. These reflected photons can in turn reach the front surface of the active region. This front surface is typically AR-coated in order to minimize the refractive index mismatch at the silicon-air interface. This increases the transmission of photons through this interface and consequently limits further potential internal reflections in the active silicon region.

However since AR coatings are not perfect, longer wavelength photons can undergo several reflections back-and-forth in the depletion region, and under conditions dictated by the cavity characteristics create destructive and constructive interferences. These multiple reflections increase the chance of NIR photons being absorbed and therefore increase the QE of the sensor in the NIR. The interference pattern linked to the wavelength-selectivity of the étalon is referred to as **spectral fringing**. Since the surfaces of the depletion region are not perfectly parallel or flat, local variations of a few μm of the depletion region thickness can change

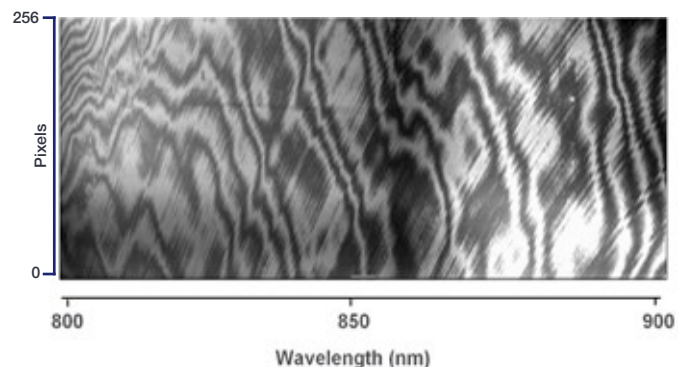


Figure 8: Un-binned image of a broadband tungsten lamp taken with a Shamrock 750 spectrograph and a back-illuminated visible-optimized iDus 420A-BV

the interference conditions and alter the spectral fringing pattern. This effect is referred to as **spatial fringing**. The detected fringing pattern on a CCD is a combination of both spectral and spatial contributions. The combined effects of spectral and spatial fringing is illustrated in Figure 8 back-illuminated sensor (BV) optimized for the visible region.

For spectroscopy applications, multiple wavelengths are dispersed across the CCD sensor width: the subsequent fringing pattern superimposed on the 'normal' signal will show the contribution of each interfering wavelength. The AR coatings applied to the front surface of the depletion region are specific to a particular wavelength range. Outside the range of greatest efficiency, the Finesse of the cavity is affected, resulting in a gradual decrease of fringe sharpness and intensity. Note: single NIR coatings applied to back-illuminated, deep depletion CCDs are typically optimized at around 800 nm, bringing the peak QE to ~95% at this wavelength.

Influence of cooling temperature

Cooling is used to minimize thermally generated 'dark noise' contribution in CCDs in order to maximise SNR. The latest generation of thermo-electric (TE) based scientific cameras can achieve sensor temperatures down to -100°C.

Cooling also has an influence on the photon absorption depth in crystalline silicon, changing the refractive index of the active region [2], while also inducing small mechanical changes in the active silicon structure. This means that the étalon characteristics also change with temperature, resulting in temperature-dependent constructive and destructive interference patterns as illustrated on Figure 9.

Maintaining a stable cooling temperature is therefore strongly recommended when dealing with relative or absolute intensity data correction, where such changes

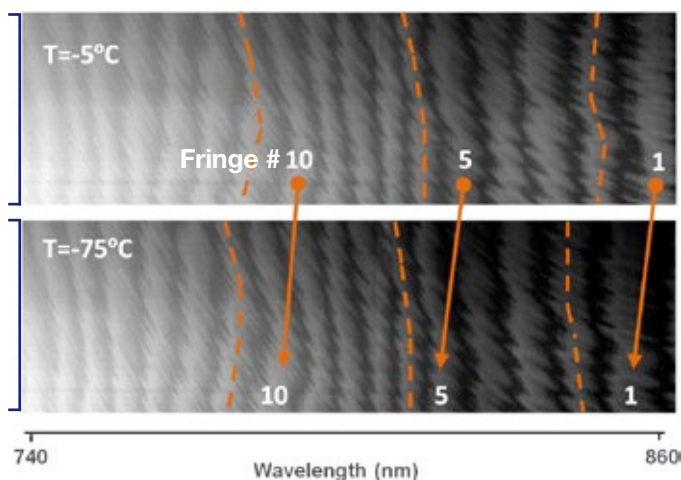


Figure 9: Un-binned images of broadband tungsten source captured with a back-illuminated visible-enhanced Newton DU971-BV EMCCD at different sensor cooling temperatures. Camera was coupled to a Shamrock 750 spectrograph. Fringes are identified by a number to facilitate visualization of the shift with temperature.

in the sensor characteristics and interference pattern will have an impact on the baseline data taken with the standard calibration source.

Minimizing etaloning in back-illuminated CCDs

Interference patterns in back-illuminated CCDs can never be totally suppressed, but can be reduced through a range of techniques highlighted here.

Front-illuminated CCDs do not suffer from optical etaloning. In these devices, incoming photons with longer absorption lengths (longer wavelengths) do not encounter any interface with highly mismatched refractive indexes after reaching the photosensitive region. These photons therefore have a very low chance of being reflected back-and-forth in the depletion region and create interferences. Photons that are not absorbed in this region are lost in the optically dead bulk silicon substrate.

Several approaches can be used to minimize etaloning in the NIR for back-illuminated CCDs:

- **Increase of the depletion region thickness** - this increases the probability for NIR photons being absorbed in the photosensitive region before being able to undergo multiple reflections and a loss in coherence due to the longer optical pathlengths.
- **Relative / absolute intensity calibration** - the use of a stable reference lamp with known emissivity characteristics can be used to correct for the optical response of a CCD camera, or the optical transfer function of an optical instrument (e.g. spectrograph, CCD cameras and light coupling optics). The term Radiometric calibration is typically used to describe an absolute spectral calibration.
- **Extensive binning to increase interference pattern averaging (spectroscopy)** - by increasing the dispersion of the signal in the 'spatial' axis (vertically) on a back-illuminated CCD coupled to the output of a spectrograph, extensive vertical binning can be used (e.g. 'full vertical binning' mode). This creates a better chance to efficiently average the signal intensity modulation linked to the alternation of constructive (peaks) and destructive (dips) interference fringes imaged across the CCD pixel columns.
- **'Fringe-suppression' process** - this refers to a CCD manufacturing process consisting of the controlled 'roughening' of the back surface of the depletion region, hence disrupting the interferometer cavity parallelism. This helps reduce the coherence within the interfering light signal.

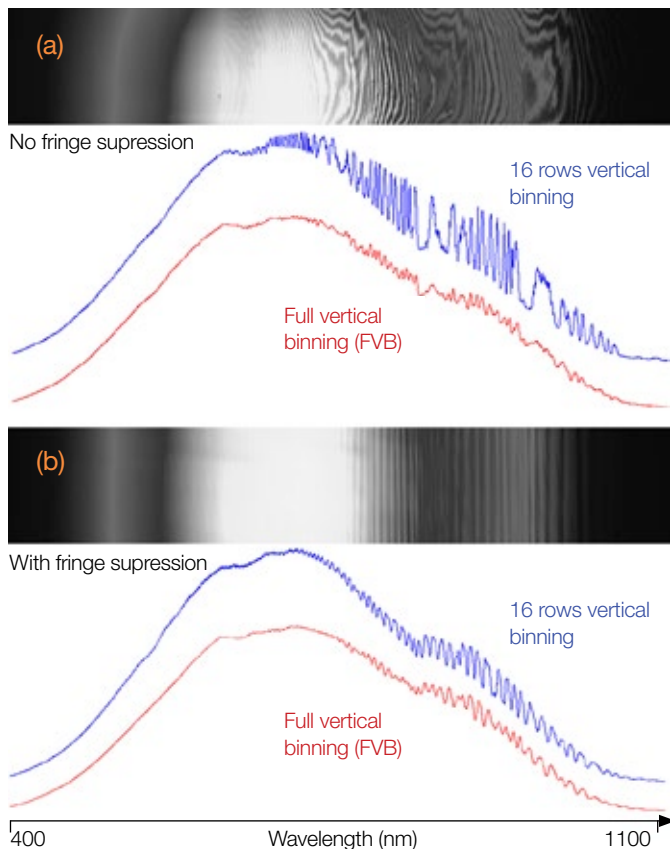


Figure 10: FVB spectra (red) and 16-row high binned track spectra (blue) of a broadband tungsten source acquired with a 'standard' back-illuminated CCD (a), and a back-illuminated CCD with 'fringe-suppression' (b) attached to a Shamrock 750 spectrograph. Corresponding un-binned images are shown above each dataset.

All of these methods are sensitive to the way light is coupled onto the CCD and to the sensor temperature.

Table 1 highlights the effectiveness of the fringe suppression process for different types of back-illuminated CCDs. It should be noted that this process intrinsically can have large variations within it.

	BI Deep-Depletion without fringe suppression	BI Deep-Depletion with fringe suppression	BI visible-enhanced without fringe suppression	BI visible-enhanced with fringe-suppression
Peak modulation in the NIR	> 10	1-5%	20-40%	10-20%

Table 1: Typical (peak - peak) signal modulation for a range of back-illuminated CCD types.

Influence of vertical binning

The modulation amplitude will also depend on the number of pixels binned on the sensor. Figure 10 shows a number of binned continuous broadband spectra in 2 binning configurations: (i) Full Vertically Binning (FVB) on a 3.2 mm high sensor, and (ii) a 16-row high binned track in the middle of the same sensor. Spectral profiles are for (a) a 'standard' back-illuminated CCD without fringe suppression (BV) and, (b) a back-illuminated with fringe suppression (BVF): both sensors are optimized for the visible region.

The following observations can be made:

- FVB spectra show little difference in terms of etaloning modulation for either 'standard' or 'fringe-suppression' CCD types. This can be explained by the effective averaging of the interference fringe modulation over a large number of rows on the CCD.
- In the case of 'Imaging Spectroscopy' (multi-track spectroscopy, hyperspectral imaging or superfast spectral acquisition modes such as Crop Mode), a limited number of CCD rows are binned at one time. The averaging of the fringe modulation is not as effective, as clearly shown on Figure 9 (16 rows vertically binned spectra). In this case the 'fringe-suppression' technology is clearly of great benefit, showing two to three times less modulation amplitude than the 'standard' back-illuminated CCD type.

Back-Illuminated deep-depletion CCDs – High NIR QE and Low etaloning

BI-DD sensors boast typical peak QE up to 95% in the NIR (see Figure 4), which makes these devices the platform of choice for low light NIR detection. But the other great advantage of such sensors is the extremely low etaloning exhibited in the NIR.

The thicker photosensitive region of BI-DD sensors offers a greater absorption path for longer wavelength photons, which minimizes the chance for multiple reflections of NIR photons occurring inside the étalon-like photosensitive region structure. This consequently greatly reduces the detected signal modulation in the NIR. In order to further reduce this signal modulation, sensor manufacturers apply a 'Fringe-suppression' process described in previous section.

Figure 11 illustrate the signal modulation in BI-DD CCDs. It clearly shows the much reduced fringing pattern on both image and vertically binned spectra compared to thinner back-illuminated CCDs (see Figure 10).

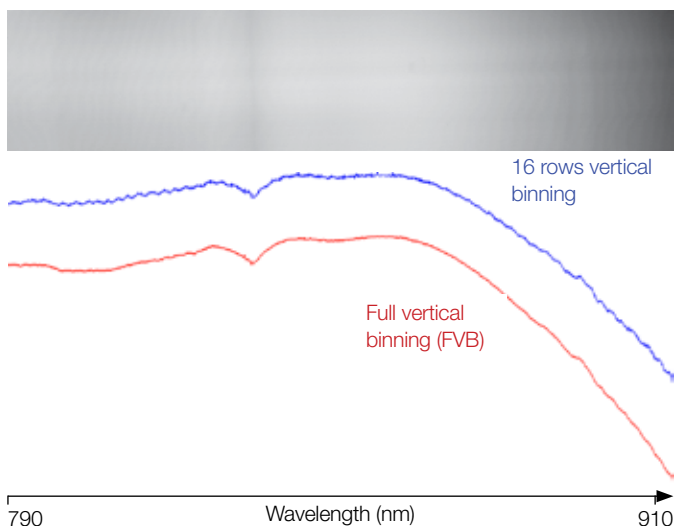


Figure 11: FVB spectra (red) and 16 rows high binned track spectra (blue) of a broadband tungsten source acquired with a back-illuminated deep-depletion CCD attached to a Shamrock 750 spectrograph.

Summary

- Optical etaloning in the NIR is an issue on any back-illuminated back-thinned CCD
- Signal modulation can be up to 40%
- Optical etaloning in the NIR is not an issue on Front-illuminated CCDs
- Optical etaloning on any back-illuminated CCD can only be minimized, never completely removed
- ‘Fringe-suppression’ technology is an effective way to reduce etaloning effects in both back-thinned CCDs optimized for the visible and deep-depletion CCDs optimized for the NIR region.
- BI-DD CCDs exhibit greatly reduced optical etaloning compared to thinner back-illuminated CCDs.

Appendix A

Key spectroscopy sensors and platforms by Andor

Andor sensor code	Description	Wavelength range (nm)	Peak QE	Fringe suppression process	Peak modulation amplitude	Dark current	Andor platform
FI	Front-illuminated	400 - 1100	58% @ 770 nm	Not necessary	0%	Very low	iDus 401, Newton 940, NewtonEM 970, NewtonEM 971
OE	Open electrode	<200 – 1100	58% @ 770 nm	Not necessary	0%	Very low	iDus 420, Newton 920
BV	Back-illuminated, Visible-optimized AR coating	<200 – 1100	97% @ 550 nm	No	20-40% (850 – 900 nm)	Low	iDus 420, Newton 920, Newton 940, NewtonEM 970, NewtonEM 971
BVF	Back-illuminated, Visible-optimized AR coating	<200 – 1100	97% @ 550 nm	Yes	10-20% (850 – 900 nm)	Low	iDus 401, iDus 420, Newton 920, NewtonEM 970
BR-DD	Back-illuminated, deep-depletion NIR-optimized AR coating	<200 – 1100	95% @ 800 nm	Yes	1-5% (~ 950 nm)	High	iDus 420, Newton 920
BEX2-DD	Back-illuminated, deep-depletion Broadband, dual AR coating	300 – 1100	93% @ 800 nm 92% @ 420 nm	Yes	1-5% (~ 950 nm)	High	iDus 420, Newton 920
LDC-DD	Back-illuminated, deep-depletion NIR-optimized AR coating	<200 – 1100	95% @ 800 nm	Yes	1-5% (~ 950 nm)	Low	iDus 416

Table 2: Summary of main front-illuminated and back-illuminated, back-thinned sensors offered by Andor

References

- [1] Sensitivity of CCD cameras – some key factors to consider. <http://www.andor.com/learning-academy/sensitivity-of-ccd-cameras-key-factors-to-consider>
- [2] Green, M.A. and Keevers, M. Optical properties of intrinsic silicon at 300 K. Progress in Photovoltaics, p.189-92, vol.3, no.3 (1995)
- [3] G. Hernandez, Fabry-Pérot interferometers, Cambridge Studies in Modern Optics, Cambridge University Press, ISBN 0-521-32238-3 (1986)
- [4] Low Dark Current Deep-Depletion (LDC-DD) Technology. [http://www.andor.com/learning-academy/low-dark-current-deep-depletion-\(lcc-dd\)-technology-a-new-standard-for-low-light-nir-spectroscopy](http://www.andor.com/learning-academy/low-dark-current-deep-depletion-(lcc-dd)-technology-a-new-standard-for-low-light-nir-spectroscopy)